JOURNAL OF CHEMICAL & ENGINEERING DATA

ARTICLE

pubs.acs.org/jced

Dynamic Interfacial Tension between Water and *n*-Octane plus Sorbitan Monolaurate at (274.2 to 293.2) K

Bao-Zi Peng,[†] Guang-Jin Chen,[*,†] Chang-Yu Sun,[*,†] Bei Liu,[†] Yan-Qin Zhang,[‡] and Qian Zhang[‡]

[†]State Key Laboratory of Heavy Oil Processing, China University of Petroleum, Beijing 102249, China

[‡]High Pressure Fluid Phase Behavior & Property Research Laboratory, China University of Petroleum, Beijing 102249, China

ABSTRACT: The equilibrium and dynamic interfacial tension of water/*n*-octane plus sorbitan monolaurate (the commercial name of Span 20) were measured using the pendant drop technique at four temperatures, (274.2, 278.2, 282.2, and 293.2) K. The concentration range of Span 20 is from (0.014 to 1.41) g·kg^{-1}. The experimental results showed that Span 20 has excellent interface activity and a pronounced dynamic effect on the water/*n*-octane interface. The critical micelle concentration of Span 20 at different temperatures was determined, and it shifts toward lower value with the increase of temperature. The dynamic interfacial tension data show that, at the beginning of the adsorption process, it was only diffusion-controlled. At the near-equilibrium stage, there exists an adsorption barrier due to the strong molecular interaction of Span 20.

INTRODUCTION

Hydrates are crystalline, ice-like solids that form when gas molecules are trapped in hydrogen-bonded water cages under high pressure and low temperature conditions.[1] Much pipeline transportation of raw hydrocarbons from wells to processing facilities is operated in the hydrate formation domain. Hydrate blockage often happens in these pipelines, and thermodynamics inhibitors such as methanol are in general added to overcome this problem. An alternative method to control gas hydrate is by adding low dosage hydrate inhibitors (LDHIs), which are divided into two main categories, kinetic inhibitors (KIs) and antiagglomerants (AAs).[2] KIs are active at low concentration, for example, w = 0.001 to 0.01, based on the water phase, and they could delay crystal growth for a certain period of time. AAs allow hydrates to form and enable them to disperse in the liquid hydrocarbon phase as small masses but prevent them from agglomerating. Since AAs are used under the existence of hydrocarbon liquid,[3] the adsorption behavior of AAs at the oil−water interface is of great importance for their development. Sorbitan monolaurate (Span 20), a kind of nonionic commercial surfactant, was tested so that it could keep hydrate particles suspended in a range of condensate types[4] and decreases the adhesion force between hydrate particles,[5] which are acting as a kind of AA. Additionally, Span 20 is also employed in the dispersion of water in water−oil nanoemulsions.[6,7] Therefore, it is necessary to investigate the adsorption behavior of Span 20 at the oil−water interface.

The equilibrium and dynamic interfacial tension are important interface properties. The equilibrium interfacial tension data for methane + KIs, such as VC713,[8] inhibex 301,[9] and inhibex 501,[9] have been reported. Rojas et al.[10] also studied the dynamic interfacial tension at the air−liquid interface after adding KI. The equilibrium interfacial tension data for methane[11] or ethylene[12] + aqueous solution of surfactant were also reported. For the oil−water interface containing AAs, interfacial tension data also provide a great deal of information concerning the adsorption of AAs. In this work, the equilibrium and dynamic interfacial tension between water and *n*-octane plus Span 20 were measured using the pendant drop technique. The effect of temperature and concentration on the interfacial properties of Span 20 at the water−*n*-octane interface and the corresponding adsorption mechanism were also discussed.

EXPERIMENTAL SECTION

Span 20 and *n*-octane of analytical grade (0.999 mass fraction) were purchased from Beijing Chemical Reagents Corporation. The molecular structure of Span 20 is shown in Figure 1. In this work, as Span 20 is insoluble in water;[13,14] it dissolved in the *n*-octane phase instead. The water used was distilled twice, and its conductivity was less than 10^{-4} S·m^{-1}. All of the materials were weighed using a balance with an accuracy of 0.0001 g.

The pendant-drop technique has been extensively used to study the dynamic interfacial tension.[15−18] In this work, the modified JEFRI pendant drop apparatus, manufactured by D. B. Robinson Corporation, was used to measure the equilibrium and dynamic interfacial tension of water−*n*-octane plus Span 20. The schematic diagram of the experimental device was shown in Figure 2.

An optical system, which consists of a zoom stereomicroscope, was installed perpendicular to the visualizing window of the high-pressure interfacial tension cell. The inner diameter and length of pendant drop cell are (3.5 and 3.0) cm, respectively. In addition, a high-resolution Panasonic photographic camera was connected to a computer for processing the photographic data using a program developed in-house.[9,11,19] The operating temperature was controlled by three Eurotherm temperature controllers with an uncertainty of ± 0.1 K. All of the pressure gauges were calibrated using a standard RUSKA dead-weight pressure gauge with an uncertainty of ± 0.25 %.

Special Issue: John M. Prausnitz Festschrift

Received: December 20, 2010
Accepted: March 1, 2011
Published: March 10, 2011

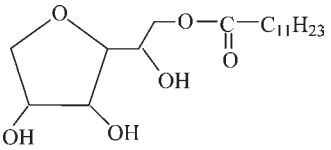

Figure 1. Molecular structure of Span 20.

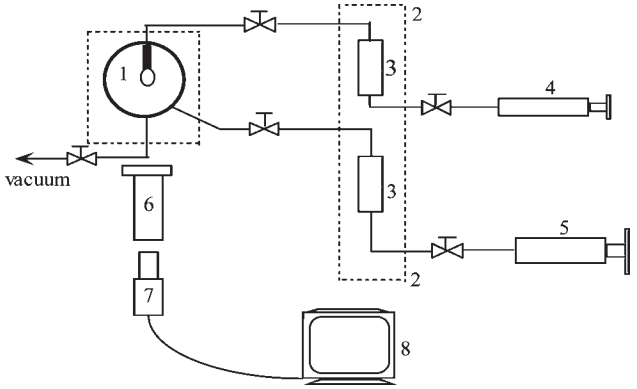

Figure 2. Schematic diagram of the experimental apparatus: 1, pendant drop cell; 2, thermostat; 3, sample cylinder; 4, motor proportioning pump; 5, JEFRI 10-1-12-NA pump; 6, microscope; 7, video camera; 8, computer.

Table 1. Equilibrium Interfacial Tension of Water−*n*-Octane at Different Temperatures and Span 20 Concentrations in *n*-Octane Phase when at 0.1 MPa

C/g·kg^{-1}	γ/mN·m^{-1}			
	T/K = 274.2	T/K = 278.2	T/K = 282.2	T/K = 293.2
0	53.14	52.68	52.21	50.92
0.014	25.24	24.69	24.26	23.01
0.028	22.45	21.43	21.61	19.40
0.042	19.19	18.38	17.87	16.38
0.056	18.01	17.36	16.87	15.12
0.070	16.77	15.64	14.72	12.85
0.084	15.50	14.46	13.53	11.48
0.098	14.60	13.40	12.65	10.51
0.14	13.25	12.03	10.56	8.36
0.28	9.80	8.93	8.13	5.65
0.42	8.54	7.41	6.67	5.65
0.56	7.87	7.40	6.67	5.66
0.70	7.86	7.41	6.66	5.65
0.84	7.87	7.41	6.67	5.66
1.41	7.86	7.41	6.66	5.65

The measurement procedure of dynamic interfacial tension is similar to that of equilibrium interfacial tension, which has been described in detail in our previous work.[9,11,19] First, the pendant-drop cell and all of the connections were soaked in petroleum ether over 3 h, and this step was repeated prior to the loading of each group of new sample. The entire system was then flushed with hot distilled water and dried with compressed air and vacuumized. Subsequently, water was added into one of the sample cylinders, and *n*-octane with a known concentration of surfactants was added into another sample cylinder and the pendant-drop cell. Then the temperature was set to the desired value. When the system temperature was stable, a water drop was pressed out and formed at the tip of the needle with a diameter of 2.032 mm. The drop of any required size could be controlled precisely within 1 s by a motor proportioning pump. Meanwhile, the timer was started, and the drop profile was magnified by the microscope and recorded by a computer through the video camera. The dimensions of the drop profile could be disposed automatically using software developed in-house. The uncertainty of the interfacial tension results mainly arises from measuring and processing the profile of pendant drop,[9] which is determined to be 0.20 mN·m^{-1}.

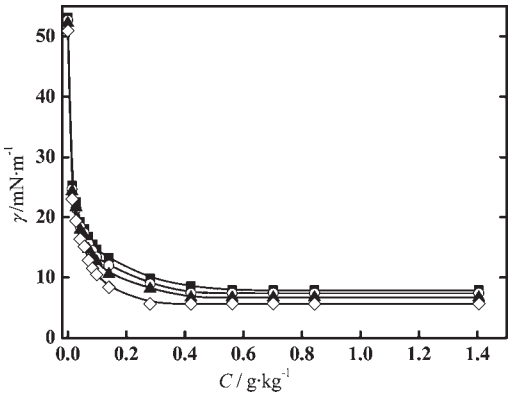

Figure 3. Equilibrium interfacial tension of water−*n*-octane plus Span 20: −■−, 274.2 K; −○−, 278.2 K; −▲−, 282.2 K; −◇−, 293.2 K.

RESULTS AND DISCUSSION

Equilibrium Interfacial Tension. The equilibrium interfacial tension is often used to describe the equilibrium properties of the surfactants, which is of importance for the adsorption study. The equilibrium interfacial tension between water and *n*-octane plus Span 20 at four temperatures and 0.1 MPa is listed in Table 1 and shown in Figure 3. The concentration range of Span 20 in *n*-octane is from (0 to 1.41) g·kg^{-1}. From Table 1 and Figure 3, it was obviously found that interfacial tension value decreases sharply after adding a small amount of Span 20 into *n*-octane. For instance, when Span 20 concentration increases from (0 to 0.056) g·kg^{-1}, the interfacial tension of water−*n*-octane plus Span 20 decreases from (53.14 to 18.01) mN·m^{-1} at 274.2 K and from (50.92 to 15.12) mN·m^{-1} at 293.2 K, indicating that Span 20 has an excellent interface activity and dynamic effect on the water−*n*-octane interface. Temperature also contributes a positive role to the decrease of equilibrium interfacial tension. It should be noticed that the equilibrium interfacial tension value hardly changes after Span 20 concentration attained a certain value at each group of temperature, showing that there exists a critical concentration for Span 20 adsorption at the water−*n*-octane interface. It is known that there include three hydroxyl groups in a Span 20 molecular as shown in Figure 1. The strong interactions (hydrogen bonding) enable Span 20 molecular to association easily, possibly causing Span 20 to form reversed micelle in *n*-octane. This may be the reason that water-in-oil emulsion forms after adding Span 20.[7,13] When Span 20 concentration reaches a critical micelle concentration (cmc), the equilibrium interfacial tension value almost remains constant

Table 2. The cmc of Span 20 for Water−*n*-Octane System

T/K	274.2	278.2	282.2	293.2
cmc/g·kg^{-1}	0.56	0.42	0.42	0.28

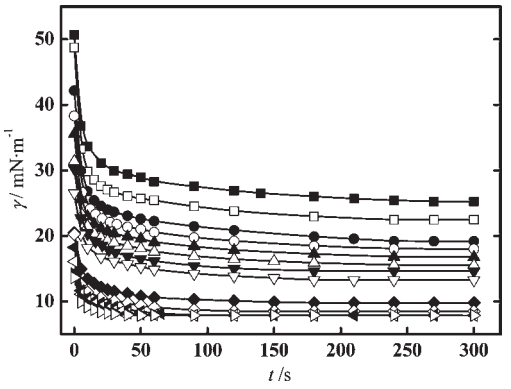

Figure 4. Dynamic interfacial tension between water and *n*-octane at various Span 20 concentrations when at 274.2 K: −■−, 0.014 g·kg^{-1}; −□−, 0.028 g·kg^{-1}; −●−, 0.042 g·kg^{-1}; −○−, 0.056 g·kg^{-1}; −▲−, 0.070 g·kg^{-1}; −△−, 0.084 g·kg^{-1}; −▼−, 0.098 g·kg^{-1}; −▽−, 0.14 g·kg^{-1}; −◆−, 0.28 g·kg^{-1}; −◇−, 0.42 g·kg^{-1}; solid left-pointing triangle, 0.56 g·kg^{-1}; open left-pointing triangle, 0.70 g·kg^{-1}; solid right-pointing triangle, 0.84 g·kg^{-1}; open right-pointing triangle, 1.41 g·kg^{-1}.

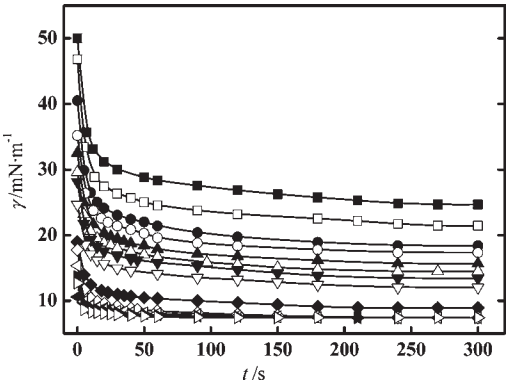

Figure 5. Dynamic interfacial tension between water and *n*-octane at various Span 20 concentrations when at 278.2 K: −■−, 0.014 g·kg^{-1}; −□−, 0.028 g·kg^{-1}; −●−, 0.042 g·kg^{-1}; −○−, 0.056 g·kg^{-1}; −▲−, 0.070 g·kg^{-1}; −△−, 0.084 g·kg^{-1}; −▼−, 0.098 g·kg^{-1}; −▽−, 0.14 g·kg^{-1}; −◆−, 0.28 g·kg^{-1}; −◇−, 0.42 g·kg^{-1}; solid left-pointing triangle, 0.56 g·kg^{-1}; open left-pointing triangle, 0.70 g·kg^{-1}; solid right-pointing triangle, 0.84 g·kg^{-1}; open right-pointing triangle, 1.41 g·kg^{-1}.

with a further increase of the concentration of Span 20, and the cmc of Span 20 in *n*-octane at different temperatures is listed in Table 2. It can be found that with the increase of temperature, the cmc shifts to a lower value.

Dynamic Interfacial Tension. Figures 4 to 7 show the dynamic interfacial tension of water−*n*-octane plus Span 20 at ambient pressure and the range of temperature from (274.2 to 293.2) K. A total of 14 groups of Span 20 concentration were examined, which range from (0.014 to 1.41) g·kg^{-1}. In comparison, the variation of trend in dynamic interfacial tension at four

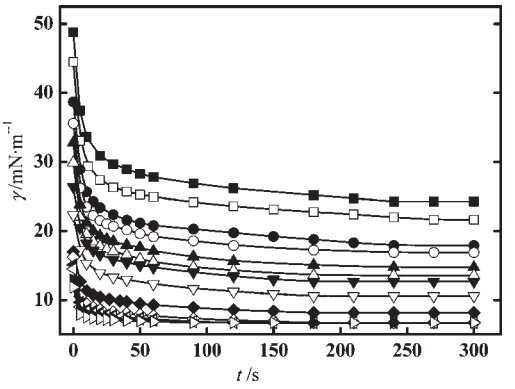

Figure 6. Dynamic interfacial tension between water and *n*-octane at various Span 20 concentrations when at 282.2 K: −■−, 0.014 g·kg^{-1}; −□−, 0.028 g·kg^{-1}; −●−, 0.042 g·kg^{-1}; −○−, 0.056 g·kg^{-1}; −▲−, 0.070 g·kg^{-1}; −△−, 0.084 g·kg^{-1}; −▼−, 0.098 g·kg^{-1}; −▽−, 0.14 g·kg^{-1}; −◆−, 0.28 g·kg^{-1}; −◇−, 0.42 g·kg^{-1}; solid left-pointing triangle, 0.56 g·kg^{-1}; open left-pointing triangle, 0.70 g·kg^{-1}; solid right-pointing triangle, 0.84 g·kg^{-1}; open right-pointing triangle, 1.41 g·kg^{-1}.

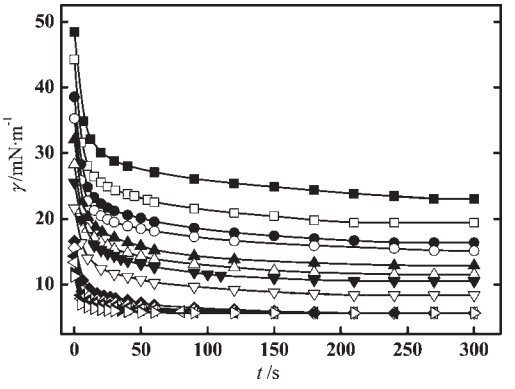

Figure 7. Dynamic interfacial tension between water and *n*-octane at various Span 20 concentrations when at 293.2 K: −■−, 0.014 g·kg^{-1}; −□−, 0.028 g·kg^{-1}; −●−, 0.042 g·kg^{-1}; −○−, 0.056 g·kg^{-1}; −▲−, 0.070 g·kg^{-1}; −△−, 0.084 g·kg^{-1}; −▼−, 0.098 g·kg^{-1}; −▽−, 0.14 g·kg^{-1}; −◆−, 0.28 g·kg^{-1}; −◇−, 0.42 g·kg^{-1}; solid left-pointing triangle, 0.56 g·kg^{-1}; open left-pointing triangle, 0.70 g·kg^{-1}; solid right-pointing triangle, 0.84 g·kg^{-1}; open right-pointing triangle, 1.41 g·kg^{-1}.

temperatures is similar to each other. From Figures 4 to 7, it can be seen that the dynamic interfacial tension value at a specified temperature reduces rapidly in the first 100 s, then followed by a gradual decrease. If at higher Span 20 concentration, the rapid reduction of dynamic interfacial tension value at the initial stage was more obvious.

Several models based on the diffusion-controlled adsorption of single nonionic surfactant have been proposed to describe the dynamic process.[20−23] Similar to Rojas et al.,[10] we used the classical Ward and Tordai equation[20] to build the relation between equilibrium interfacial tension and dynamic interfacial tension. This equation accounted for the diffusion of monomers from the bulk to the interface and was given as follows:

$$\Gamma(t) = 2C_0\left(\frac{Dt}{\pi}\right)^{1/2} - 2\left(\frac{D}{\pi}\right)^{1/2}\int_0^{\sqrt{t}} C_s d(\sqrt{t-\tau}) \qquad (1)$$

dx.doi.org/10.1021/je101094u |*J. Chem. Eng. Data* 2011, 56, 1617–1621

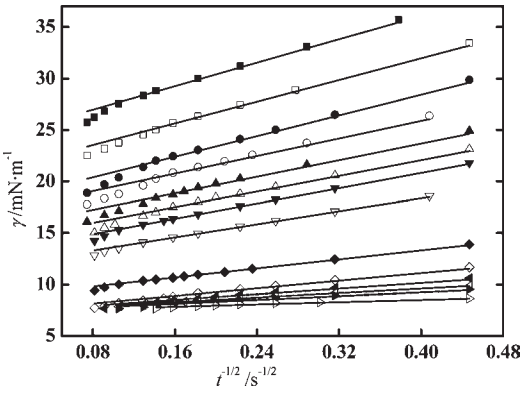

Figure 8. Dynamic interfacial tension plotted as $t^{-1/2}$ at water−*n*-octane plus Span 20 interface when at 278.2 K. The Span 20 concentration is as follows: ■, 0.014 g·kg^{-1}; □, 0.028 g·kg^{-1}; ●, 0.042 g·kg^{-1}; ○, 0.056 g·kg^{-1}; ▲, 0.070 g·kg^{-1}; △, 0.084 g·kg^{-1}; ▼, 0.098 g·kg^{-1}; ▽, 0.14 g·kg^{-1}; ◆, 0.28 g·kg^{-1}; ◇, 0.42 g·kg^{-1}; solid left-pointing triangle, 0.56 g·kg^{-1}; open left-pointing triangle, 0.70 g·kg^{-1}; solid right-pointing triangle, 0.84 g·kg^{-1}; open right-pointing triangle, 1.41 g·kg^{-1}; —, calculated line by eq 5.

where $\Gamma(t)$ is the dynamic adsorption density, C_0 is the bulk surfactant concentration, D is the diffusion coefficient, C_s is the subsurface concentration, τ is a dummy variable of integration, $\pi = 3.142$, and t is the pendant drop hold time.

At the start of the adsorption process the subsurface concentration is small and is neglected, yielding:

$$\Gamma(t) = 2C_0\sqrt{\frac{Dt}{\pi}} \quad (2)$$

After a long time, the adsorption has nearly attained equilibrium, and the subsurface concentration changes little with time; eq 1 approximates to:

$$\Gamma(t) = 2\sqrt{\frac{4Dt}{\pi}}\Delta C^s \quad (3)$$

where $\Delta C^s = C_0 - C_s$.

If the adsorption process is diffusion-controlled, this change in subsurface concentration ΔC^s corresponds to a change in interfacial tension:

$$\gamma(t) - \gamma_e = \frac{d\gamma}{dC}\Delta C^s \quad (4)$$

where $\gamma(t)$ and γ_e are the dynamic and equilibrium interfacial tension, respectively. Combining with Gibbs equation and eq 2, the long time approximation can be written in the following form:

$$\gamma(t) = \gamma_e + \frac{RT\Gamma_e^2}{C_0}\sqrt{\frac{\pi}{4Dt}} \quad (5)$$

where Γ_e is the equilibrium adsorption density.

To investigate the adsorption mechanism of Span 20 at the water−*n*-octane interface, eq 5 was applied to analyze the experimental data before the interfacial tension value attains a plateau region. Figure 8 shows the plot of interfacial tension with inverse of square root of pendant drop formation time at 278.2 K. It can be found that at the beginning of the adsorption process, $\gamma(t)$ and $t^{-1/2}$ are in an excellent linear relationship, while it deviates obviously from the straight line at the end of adsorption process. This result indicates that the adsorption process at the initial stage is only diffusion-controlled. However, there is no more simple diffusion control at the near-equilibrium stage. It also shows that there exists an adsorption barrier for Span 20 from subsurface to interface, which may result from the molecular interaction of Span 20. With the proceeding of adsorption, the diffusion of Span 20 was restrained due to the strong molecular interaction and incurs the adsorption barrier.

CONCLUSIONS

The equilibrium and dynamic interfacial tension of water−*n*-octane plus Span 20 were measured using the pendant-drop apparatus. The experimental results show that a small amount of Span 20 in *n*-octane is capable of decreasing water−*n*-octane interfacial tension significantly. The temperature also contributes a positive role to the decrease of equilibrium interfacial tension. A critical concentration for Span 20 adsorption at the water−*n*-octane interface was also determined, and it shifts to a lower value with the increase of temperature. The dynamic interfacial tension value at a specified temperature reduces rapidly at the initial stage and then decreases slowly. A diffusion-controlled model was applied to investigate the adsorption mechanism of Span 20 at the water−*n*-octane interface. The results confirmed that, at the beginning of the adsorption process, it was only diffusion-controlled, but there is no more simple diffusion control at the near-equilibrium stage.

AUTHOR INFORMATION

Corresponding Author

*Fax: +86 10 89732126. E-mail: gjchen@cup.edu.cn (G. J. Chen); cysun@cup.edu.cn (C. Y. Sun).

Funding Sources

The financial support received from the National Natural Science Foundation of China (Nos. 20925623, 21076225), National 863 Project, Targeted Advanced Item of China University of Petroleum (QZDX-2010-02), and National 973 Project of China (No. 2009CB219504) is gratefully acknowledged.

REFERENCES

(1) Sloan, E. D.; Koh, C. A. *Clathrate Hydrate of Natural Gases*, 3rd ed.; CRC Press: Boca Raton, FL, 2007.

(2) Kelland, M. A. History of the Development of Low Dosage Hydrate Inhibitors. *Energy Fuels* **2006**, *20*, 825–847.

(3) Swanson, T. A.; Petrie, M.; Sifferman, T. R. In *the Successful Use of both Kinetic Hydrate and Paraffin Inhibitors together in a Deepwater Pipeline with a High Water Cut in the Gulf of Mexico*, Proceedings of the 2005 SPE International Symposium on Oilfield Chemistry, Houston, Texas, USA, February 2−4, 2005; SPE 93158.

(4) Huo, Z.; Freer, E.; Lamar, M.; Sannigrahi, B.; Knauss, D. M.; Sloan, E. D. Hydrate Plug Prevention by Anti-agglomeration. *Chem. Eng. Sci.* **2001**, *56*, 4979–4991.

(5) Taylor, C. J.; Dieker, L. E.; Miller, K. T.; Koh, C. A.; Sloan, E. D. Micromechanical Adhesion Force Measurements between Tetrahydrofuran Hydrate Particles. *J. Colloid Interface Sci.* **2007**, *306*, 255–261.

(6) Porras, M.; Solan, C.; Gonzalez, C.; Martinez, A.; Guinart, A.; Gutierrez, J. M. Studies of Formation of W/O Nano-emulsions. *Colloids Surf., A* **2004**, *249*, 115–118.

(7) Porras, M.; Solans, C.; Gonzalez, C.; Gutierrez, J. M. Properties of Water-in-oil (W/O) Nano-emulsions Prepared by a Low-energy Emulsification Method. *Colloids Surf., A* **2008**, *324*, 181–188.

(8) Peng, B. Z.; Sun, C. Y.; Liu, P.; Liu, Y. T.; Chen, J.; Chen, G. J. Interfacial Properties of Methane/Aqueous VC-713 Solution under Hydrate Formation Conditions. *J. Colloid Interface Sci.* **2009**, *336*, 738–742.

(9) Liu, P.; Sun, C. Y.; Peng, B. Z.; Chen, J.; Chen, G. J. Measurement of Interfacial Tension between Methane and Aqueous Solution Containing Hydrate Kinetic Inhibitors. *J. Chem. Eng. Data* **2009**, *54*, 1836–1839.

(10) Rojas, Y. V.; Phan, C. M.; Lou, X. Dynamic Surface Tension Studies on Poly (N-vinylcaprolactam/N-vinylpyrrolidone/N,N-dimethylaminoethyl methacrylate) at the Air−liquid Interface. *Colloids Surf., A* **2010**, *355*, 99–103.

(11) Sun, C. Y.; Chen, G. J.; Yang, L. Y. Interfacial Tension of Methane + Water with Surfactant near the Hydrate Formation Conditions. *J. Chem. Eng. Data* **2004**, *49*, 1023–1025.

(12) Luo, H.; Sun, C. Y.; Huang, Q.; Peng, B. Z.; Chen, G. J. Interfacial Tension of Ethylene and Aqueous Solution of Sodium Dodecyl Sulfate (SDS) in or near Hydrate Formation Region. *J. Colloid Interface Sci.* **2006**, *297*, 266–270.

(13) Zadymova, N. M.; Karmasheva, N. V.; Poteshnova, M. V.; Tsikurina, N. N. New Procedure for Determining the Solubility of Lypophilic Nonionic Surfactants in Water. *Colloid J.* **2002**, *64*, 400–405.

(14) Lee, H. J.; Chim, B. D.; Yang, S. M.; Park, O. O. Surfactant Effect on the Stability and Electrorheological Properties of Polyaniline Particle Suspension. *J. Colloid Interface Sci.* **1998**, *206*, 424–438.

(15) Touhami, Y.; Neale, G. H.; Hornof, V.; Khalfalah, H. A Modified Pendant Drop Method for Transient and Dynamic Interfacial Tension Measurement. *Colloids Surf., A* **1996**, *112*, 31–41.

(16) Ferrari, M.; Liggieri, L.; Ravera, F.; Amodio, C.; Miller, R. Adsorption Kinetics of Alkylphosphine Oxides at Water/Hexane Interface. *J. Colloid Interface Sci.* **1997**, *186*, 40–45.

(17) Yang, D. Y.; Tontiwachwuthikul, P.; Gu, Y. G. Dynamic Interfacial Tension Method for Measuring Gas Diffusion Coefficient and Interface Mass Transfer Coefficient in a Liquid. *Ind. Eng. Chem. Res.* **2006**, *45*, 4999–5008.

(18) Wang, K.; Lu, Y. C.; Xu, J. H.; Luo, G. S. Determination of Dynamic Interfacial Tension its Effect on Droplet Formation in the T-Shaped Microdispersion Process. *Langmuir* **2009**, *25*, 2153–2158.

(19) Sun, C. Y.; Chen, G. J. Measurement of Interfacial Tension for the CO_2 Injected Crude Oil + Reservoir Water System. *J. Chem. Eng. Data* **2005**, *50*, 936–938.

(20) Ward, A. F. H.; Tordai, L. Time-Dependence of Boundary Tensions of Solutions I. The Role of Diffusion in Time-effects. *J. Chem. Phys.* **1946**, *14*, 453–461.

(21) Joos, P.; Fang, J. P.; Serrien, G. Comments on Some Dynamic Surface Tension Measurements by the Dynamic Bubble Pressure Method. *J. Colloid Interface Sci.* **1992**, *151*, 144–149.

(22) Rosen, M. J.; Gao, T. Dynamic Surface Tension of Aqueous Surfactant Solutions 5. Mixtures of Different Charge Type Surfactants. *J. Colloid Interface Sci.* **1995**, *173*, 42–48.

(23) Campanelli, J. R.; Wang, X. H. Dynamic Interfacial Tension of Surfactant Mixtures at Liquid-liquid Interfaces. *J. Colloid Interface Sci.* **1999**, *213*, 340–351.